JOURNAL OF SOLID STATE CHEMISTRY 119, 76–79 (1995)

Calculation of Electronic States in Perovskite-Type Oxide by the DV-Xα Method: The Effects of Oxygen Defects

Kouichi Goto, Fumio Munakata, and Mitsugu Yamanaka

Nissan Research Center, Nissan Motor Co., Ltd.,
1, Natsushima-cho, Yokosuka 237, Japan

and

Hirohiko Adachi

Faculty of Engineering, Kyoto University,
Yoshidahon-cho, Sakyo-ku, Kyoto, 606-01, Japan

Received November 21, 1994; in revised form March 2, 1995; accepted March 28, 1995

The effects of oxygen defects on the electronic states in the perovskite-type oxide, $SrCoO_{3-\delta}$, were investigated by the DV-Xα molecular orbital method. The oxygen-defect model was constructed on the basis of the brownmillerite-type structure. We calculated four kinds of cluster models, corresponding to $\delta = 0$, $\frac{1}{8}$, $\frac{1}{3}$, and $\frac{1}{2}$. The calculated energy of O1s state in $SrCoO_{3-\delta}$ splits into two levels with the energy difference of 2 eV, which is consistent with the experimented results in $La_{1-x}Sr_xCoO_{3-\delta}$ by X-ray photoelectron spectroscopy. © 1995 Academic Press, Inc.

1. INTRODUCTION

Perovskite-type oxides (ABO_3) are interesting materials, changing their properties drastically by the substitution of metal ions for other metal ions at *A* and/or *B* sites. In $La_{1-x}Sr_xCoO_3$, the partial Sr substitution for La exhibits high activity as oxygen electrodes (1) and oxidation catalyst (2). Recently the electronic structures of $La_{1-x}Sr_xCoO_3$ have been investigated intensively. Seiyama and co-workers observed the splitting of the O1*s* peak in $La_{1-x}Sr_xCoO_3$ using X-ray photoelectron spectroscopy (XPS) (3). They assigned the peak with lower binding energy to the lattice oxygen and that with high binding energy to the oxygen weakly bound to the surface (3). Richter *et al.* claimed that the origin of the high binding energy state was the absorbed hydroxyl or oxygen bound to La_2O_3 or SrO (4). Tabata and Matsumoto showed the possibility that it was due to the surface composition which was different from the bulk composition (5). Thus, the origin of the splitting of the O1*s* state in $La_{1-x}Sr_xCoO_3$ is considered to be unclear yet.

On the other hand, the partial Sr substitution for La causes the oxidation of Co^{3+} to Co^{4+} and the formation of O^{2-} vacancies (6). Then we assumed that the origin of O1*s* splitting may be not only the surface states but also the oxygen defects, and we applied the DV-Xα cluster calculation method with the oxygen-defect model to investigate the origin of O1*s* splitting in $La_{1-x}Sr_xCoO_{3-\delta}$.

Previously, the DV-Xα cluster calculation method was applied to oxides including perovskites (7) and several cases of oxygen-defect models, such as TiO_2 (8) and NbO (9). However, oxygen defects in the perovskite-type oxides have not been investigated by the DV-Xα method yet.

In the present paper, we report the application of the the DV-Xα method to the investigation of the oxygen defects in the perovskite-type oxide, $La_{1-x}Sr_xCoO_3$, and discuss the calculated results in comparison with the reported experimental data by XPS measurement.

2. CALCULATION METHOD

The DV-Xα method is the molecular orbital cluster method, using a local one electron effective potential to approximate the exchange correlation effect. The exchange potential V_{xc} is given by the following formula

$$V_{xc} = -3\alpha[\tfrac{3}{8}\rho]^{1/3}, \qquad [1]$$

where ρ is the electronic density. The parameter α was fixed at 0.7 in the present calculation. The calculation was carried out by CRAY-YMP8.

We made the following simplifications to calculate the electronic state of $La_{1-x}Sr_xCoO_{3-\delta}$ with oxygen defects: (i) $SrCoO_{3-\delta}$ was used instead of $La_{1-x}Sr_xCoO_{3-\delta}$, (ii) the crystal structure was assumed not to deform by the intro-

0022-4596/95 $12.00

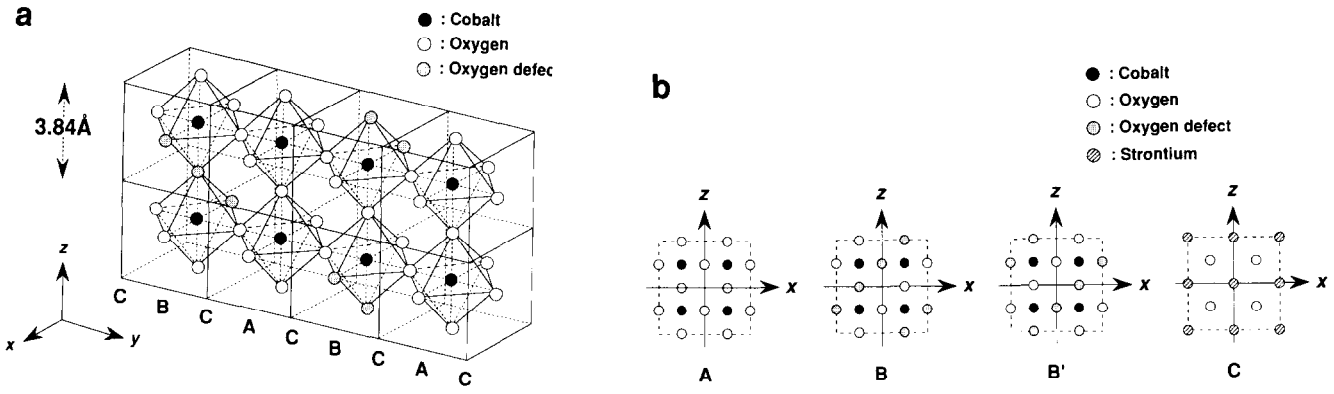

FIG. 1. (a) Calculated structure of $SrCoO_{5/2}$, which shows the half of the $Sr_5Co_{16}O_{56}$ model. A, B, B′, and C denote the zx planes with the different configuration. Strontium atoms locate on all the corners of the small cubic lattice. (b) The configuration of the atoms on the zx planes, A, B, B′, and C.

duction of oxygen defects (i.e., the distance between Co and O was the same as the value of $SrCoO_3$, 0.384 nm (9)), and (iii) the effects of the local bond states (the color centers) were ignored.

$LaCoO_3$ shows the low-spin state below room temperature and the high-spin state above it (10); we calculated low-spin and high-spin configurations of $SrCoO_{3-\delta}$.

The oxygen-defect structure in $SrCoO_{5/2}$ ($SrCoO_{3-\delta}$, $\delta = \frac{1}{2}$) was constructed on the basis of the brownmillerite-type oxide, $Ca_2Fe_2O_5$ (11). The oxygen defects in the structure are symmetrically ordered. The cluster model $Sr_5Co_{16}O_{56}$ was shown in Fig. 1. The actual model $Sr_5Co_{16}O_{56}$ consists of two clusters which are shown in Fig. 1a, connected in the x direction. Five strontium atoms in the y direction were taken into account in the calculation. Figure 1b shows the configuration of the atoms on the zx planes. A, B, and C planes show the equivalent zx planes. On the A plane, cobalt and oxygen atoms were located without defects. On the B or B′ plane, oxygen defects were induced in a straight line. On the C plane, oxygen atoms and strontium point charges were located.

To investigate structures with fewer oxygen defects, $SrCoO_{8/3}$ ($\delta = \frac{1}{3}$), $SrCoO_{17/6}$ ($\delta = \frac{1}{6}$), and $SrCoO_3$ ($\delta = 0$) were calculated. The $SrCoO_{8/3}$ model was constructed on the basis of $Sr_2LaFe_3O_8$ (11). The oxygen defects are easily introduced and modeled by decreasing the number of the B plane with oxygen defects in brownmillerite-type $SrCoO_{5/2}$. $SrCoO_{17/6}$ ($\delta = \frac{1}{6}$) model was constructed in the same way as the construction of $SrCoO_{8/3}$ model. $SrCoO_{8/3}$ and $SrCoO_{17/6}$ models are shown in Figs. 2 and 3.

A Madelung potential was also taken into account in the calculation by the summation of the point charge Coulomb potential (12). The point charge of strontium atoms was assumed to be +2e, that of oxygen to be −2e, and that

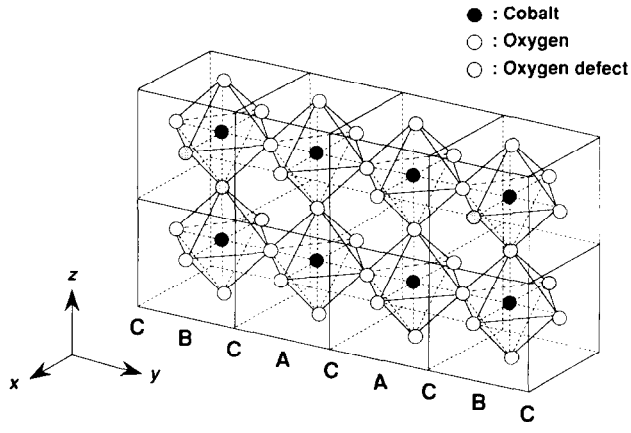

FIG. 2. Calculated structure of oxygen-deficient $SrCoO_{8/3}$, which shows half of the $Sr_5Co_{16}O_{44}$ model. Strontium atoms locate on all the corners of cubic unit cells. On the B plane, oxygen defects are induced the same as in Fig. 1b.

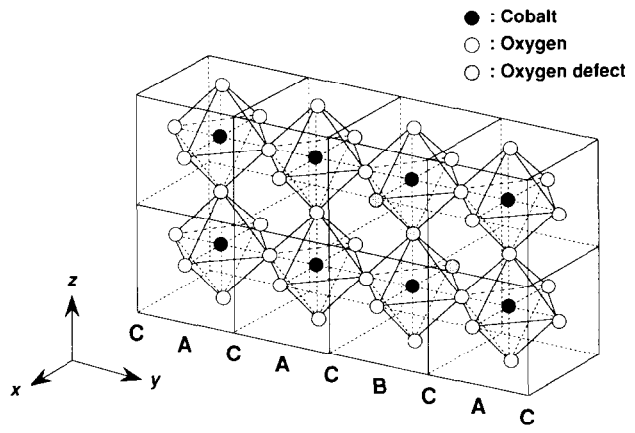

FIG. 3. Calculated structure of oxygen-deficient $SrCoO_{17/6}$, which shows half of the $Sr_5Co_{16}O_{50}$ model. Strontium atoms locate on all the corners of cubic unit cells. On the B plane, oxygen defects are induced the same as in Fig. 1b.

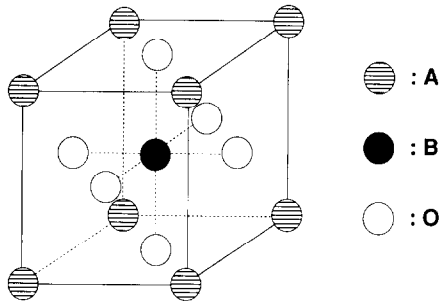

FIG. 4. Basic cubic structure (unit cell) of a perovskite oxide ABO_3. *A*, La, Sr, etc.; *B*, Co, Fe, Ni, etc; O, oxygen.

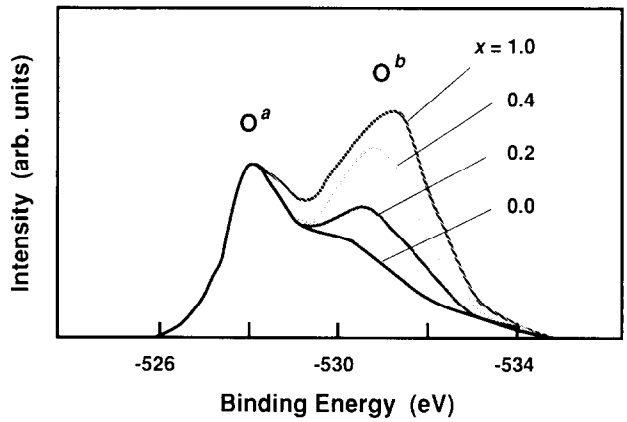

FIG. 5. XPS spectra of O1*s* states in $La_{1-x}Sr_xCoO_{3-\delta}$.

of the oxygen defect to be neutral. The charge of cobalt atom was decided by the electric neutral condition: +3e in $SrCoO_{5/2}$, $+\frac{10}{3}$ e in $SrCoO_{8/3}$, and $+\frac{11}{3}$ e in $SrCoO_{17/6}$. We distributed the point charges, the number of which corresponded to two unit cells, symmetrical around the cluster model.

3. RESULTS AND DISCUSSIONS

First, we show the calculated results using the cluster model shown in Fig. 4 to demonstrate the accuracy of the present calculation method. The experimental (3) and calculated O1*s* orbital energies are summarized in Table 1. The experimental value, i.e., −528.0 eV corresponds to the 1*s* energy of lattice oxygen (O^a) in Fig. 5 (3). The calculated O1*s* energy was converted by the transition state method (13) to about −527.5 eV measured from the energy level of HOMO. Then the energy difference between the experimental and calculated O1*s* levels was only 0.5 eV. Therefore, the present calculation method is concluded to be able to calculate the O1*s* state in the perovskite-type oxides with high accuracy.

The calculated charges by Mulliken population analysis are shown in Table 2. The calculated strontium charge is +1.98e, which is very close to the designed charge, +2e.

TABLE 1
Ionization Energies (in eV) Calculated Using $SrCoO_3$ Model Cluster

	Orbital energy (up/down)	Transition state energy (up/down)	Experimental value (2)
Co 2*p*	−765.3/−763.2	−785.8/−784.1	−780.0
O 1*S*	−503.2/−503.2	−529.4/−529.4	−528.0
HOMO	−2.2/−2.0	—	—
LUMO	+9.0/−1.0	—	—

Note. High-spin states were considered. For comparison, the experimental values obtained by XPS measurement were also shown.

Therefore, when all strontium atoms in the cluster model are replaced by +2 point charge, there is little change in the calculated result.

Next, we show the calculated results using the oxygen-defect model clusters . The calculated results of the high-spin configuration of $SrCoO_{3-\delta}$ were almost the same with the low-spin configuration, so we discuss the calculated results of the high-spin configuration. The O1*s* energy levels of each oxygen-defect model are summarized in Table 3, where oxygen atoms at the edge of the cluster model were out of consideration. O1*s* energy states in $SrCoO_{3-\delta}$ were shown as density of state (DOS) curves in Fig. 6. The DOS was obtained by convolution of the molecular orbital levels using Gaussians with FWHM 0.5 eV, after HOMO was shifted to 0 eV. The obtained DOS curves fit the experimental XPS results in Fig. 5, except for the absolute values and the energy gap of two O1*s* peaks.

The absolute value of the O1*s* energy is about 28 eV lower than the experimental data; however, the lower state corresponds to the O1*s* state with the experimental value −528.0 eV, as already mentioned.

The energy gaps of two calculated O1*s* peaks are smaller than the experimental values, 4 eV (3) and 3 eV (5). This result may be due to the neglected structural deformation caused by the substitution of Sr atoms for La atoms.

TABLE 2
Electronic Charges (in e) of the Atoms in $SrCoO_3$ Obtained by Mulliken Population Analysis

	Designed	Calculated
Sr	+2	+1.98
Co	+4	+2.64
O	−2	−1.79

TABLE 3
Calculated Ionization Energies (in eV) of Oxygen Atoms Using the $SrCoO_{3-\delta}$ Model Clusters

$\delta = 0$		$\delta = \frac{1}{6}$		$\delta = \frac{1}{3}$		$\delta = \frac{1}{2}$	
A	—	C″	—	C′	—	C	—
C	(−513.5)	A′	(−505.2)	A	(−499.7)	B′	(−500.4)
A	−514.5	C′	−505.6	C	−498.7	C	−502.3
C	−514.4	A	−505.6	A	−498.8	A	−500.4
A	−514.7	C	−508.2	C	−500.9	C	−502.4
C	−514.5	B	−505.6	B	−498.8	B	−500.3
A	−514.7	C	−508.3	C	−500.9	C	−502.4
C	−514.4	A	−505.6	A	−498.8	A	−500.4
A	−514.3	C′	−505.6	C′	−498.7	C	−502.4
C	(−513.4)	A′	(−505.3)	A	(−499.9)	B′	(−500.4)
A	—	C″	—	C	—	C	—
HOMO	−12.30		−3.04		+3.69		+2.04
LUMO	−12.28		−3.00		+3.70		+2.05

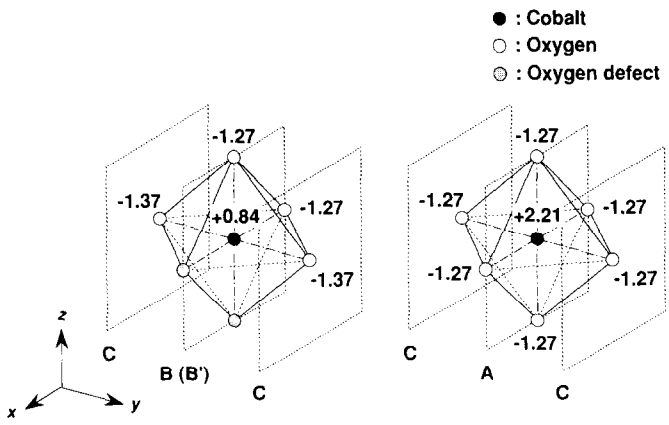

FIG. 7. Electronic charges of oxygen electrons in $SrCoO_{3-\delta}$ obtained by Mulliken population analysis.

Therefore, we consider that the origin of the splitting of the O1*s* state is the introduction of the oxygen defects in $La_{1-x}Sr_xCoO_{3-\delta}$.

The calculated charges by Mulliken population analysis are shown in Fig. 7. Two kinds of oxygen atoms were found. One is the oxygen atom with −1.37e. The other is oxygen atom with −1.27e . The former oxygen atoms locate on the C plane, adjoin the oxygen defects on the B plane, and are considered to correspond to the oxygens with the higher energy (O^b) in Fig. 6. On the other hand, the latter oxygen atoms locate on the C plane without the adjoining oxygen defect, or locate on the A or B plane . These corresponded to the oxygens with lower energy (O^a) in Fig. 6. Therefore, the excess electrons are considered to flow into the former kind of oxygens from the oxygen defects. This electron transfer may stabilize the former kind of the oxygens atoms, the 1*s* state of which is shifted to the higher binding energy than the others.

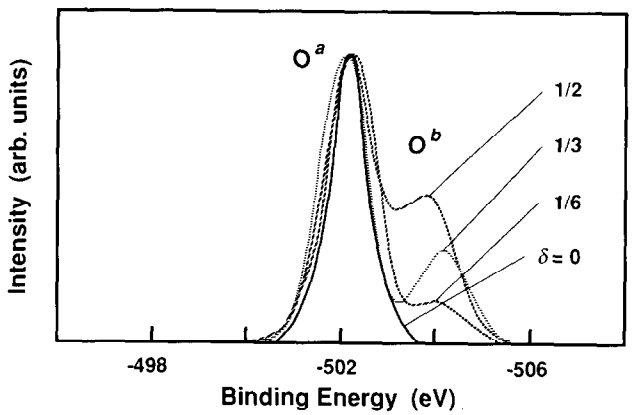

FIG. 6. Calculated density of states of O1*s* level in $SrCoO_{3-\delta}$. HOMO was shifted to 0 eV.

4. CONCLUSION

The origin of the splitting of the O1*s* state observed in $La_{1-x}Sr_xCoO_{3-\delta}$ by XPS measurement was investigated by the DV-Xα molecular orbital calculation method. Even though we use several simplifications in the calculation, the calculation showed the possibility that the origin of the splitting is considered to be due to the oxygen defects. Further investigation of the effects of the oxygen defects on the electronic structures in the perovskite-type oxide should be conducted.

REFERENCES

1. H.Obayashi and T.Kudo, *Mater. Res. Bull.* **13,** 1409 (1978).
2. T. Nakamura, M. Misono, and T. Gejo, *J. Catal.* **83,** 151 (1983).
3. N. Yamazoe, Y. Teraoka, and T. Seiyama, *Chem. Lett.*, 1767 (1981).
4. L. Richter, S. D. Bader, and M. Bbrodsky, *Phys. Rev. B* **22,** 3059 (1980).
5. K. Tabata and I. Matsumoto, *J. Mater. Sci.* **22,** 1882 (1987).
6. R. J. H. Voorhoeve, "Advanced Materials in Catalysis," p. 129. Academic Press, New York/London, 1977.
7. I. Kojima, H. Adachi, and I. Yasumori, *Surf. Sci.* **130,** 50 (1983).
8. M. Tsukuda, C. Satoko, and H. Adachi, *J. Phys. Soc. Jpn.* **47,** 1610 (1979).
9. JCPDS 38-1148, unpublished manuscript.
10. M. Abbate, J. C. Fuggle, A. Fujimori, L. H. Tjeng, C. T. Chen, R. Potze, G. A. Sawatzky, H. Eisaki, and S. Uchida, *Phys. Rev. B* **47** 16124 (1993).
11. P. D. Battle, T. C. Gibb, and P. Lightfoot, *J. Solid State. Chem.* **84,** 237 (1990).
12. H. M. Evjen, *Phys. Rev.* **39,** 1333 (1932).
13. J. C. Slater, "Quantum Theory of Molecule and Solids," Vol 4. McGraw-Hill, New York, 1974.